



UNIVERSITETET I AGDER

**Spectrum Cartography using Adaptive Multi-kernels
– Experimental validation**

Henning Idsøe

Supervisors

Prof. Linga Reddy CENKERAMADDI

Prof. Baltasar Beferull LOZANO

Dr. Mohamed HAMID

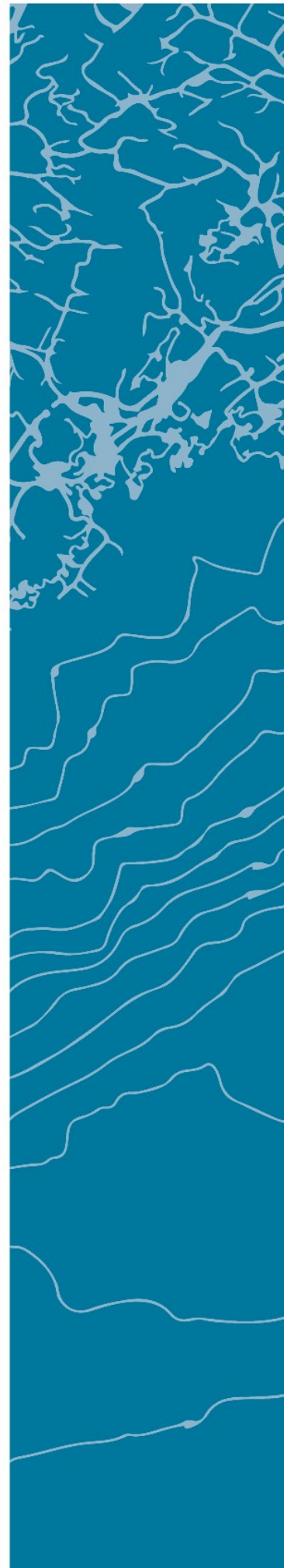
University of Agder, 2017

Faculty of engineering and science

Intelligent Signal Processing & Wireless Networks (WISENET) Lab



WISENET



Contents

| | | |
|----------|---|-----------|
| 1 | Background | 3 |
| 1.1 | Cognitive Radio | 5 |
| 1.2 | Radio Environment Maps | 5 |
| 2 | Objective | 6 |
| 3 | Function estimation | 7 |
| 3.1 | One parameter | 7 |
| 3.2 | Several parameters | 7 |
| 3.3 | Kernel methods | 9 |
| 3.4 | Gaussian Radial Basis functions | 9 |
| 3.5 | Non-Parametric Spectrum Cartography using Adaptive Radial Basis Functions | 10 |
| 4 | Detection of signal presence | 13 |
| 5 | Sequential measurements using 1 transmitter and 1 receiver | 14 |
| 5.1 | Equipment and setup | 14 |
| 5.2 | Implementation in NI LabView | 15 |
| 5.3 | Measurements and estimation | 17 |
| 6 | Parallell measurements using 14 receivers and 1 transmitter | 19 |
| 6.1 | Equipment | 19 |
| 6.1.1 | NI USRP-2953R & NI USRP-2952R | 19 |
| 6.1.2 | NI PXIe-1082 & NI PXIe-1071 | 19 |
| 6.1.3 | NI PXIe-8880 | 20 |
| 6.1.4 | NI PXIe-8374 extension card | 20 |
| 6.1.5 | NI Linux Real-Time OS | 20 |
| 6.1.6 | Ni LabVIEW Communications System Design Suite 2.0 | 21 |
| 6.2 | Implementation in Communications Suite 2.0 | 21 |
| 6.2.1 | Signal registration | 21 |
| 6.2.2 | Adaptive Radial Basis Function | 22 |
| 6.3 | Setup of measurement array | 24 |
| 6.4 | Estimation with one transmitter inside receiver array | 26 |
| 6.5 | Estimation with one transmitter outside of receiver array | 28 |
| 6.6 | Estimation based tracking of one transmitter | 31 |
| 7 | Parallell measurements with an added transmitter | 32 |
| 7.1 | Estimation for multiple transmitter setup | 32 |
| 7.2 | Estimation based tracking of multiple transmitters | 34 |
| 8 | Conclusion | 35 |
| 9 | References | 36 |
| | List of Figures | 37 |

1 Background

In 1888, Heinrich Hertz initiated the start of the wireless communications era. Using a simple apparatus and producing an electrical spark at one place, another spark appeared at a second apparatus across the room with no physical connection between them.

Hertz did not care much for the discovery, thought it was of little use. He had proved the theory of electromagnetism published by James Maxwell in 1865, and that was that.

In 1902, Guglielmo Marconi did the first radio transmission across the Atlantic Ocean. He was interested in wireless communication from a young age, and became inspired when learning of Hertz discovery of radio waves. Doing experiments and developing equipment he made it possible to communicate over longer and longer distances. Marconi is often referred to as the inventor of radio.

Today wireless communication is a part of nearly every aspect of our everyday life in the industrialized world. People uses mobiles to wirelessly communicate with each other, to stay connected to the internet and even monitor bodily functions like heartrate by sensors attached to the body. GPS services provides positioning services using radio waves sent from satellites in space, and we even send probes through the solar system which transmits back pictures and data about remote planets.

All this radio communication, although not visible to the naked eye, depends on one vital resource. Radio communication uses electromagnetic waves, and both transmitter and receiver must be set to use the same frequency. For the duration of the transmission, the transmitter should have exclusive rights to the given frequency to avoid interference and corruption of the signal at the receiving end.

To perform several simultaneous transmissions, other transmitter/receiver pairs could be tuned to other frequencies, and if there is a sufficient distance to other transmitters the frequency can be re-used. Modern communication protocols typically use a frequency range, specified by a center frequency and a bandwidth.

To avoid everyone causing interference for everyone else governments manage the frequencies and supplies licenses to those interested in using radio for communication. Some frequencies may be reserved for special purposes and some may be available for general use, such as the Industrial, Scientific and Medical (ISM) bands.

Most electronic consumer products having wireless capabilities typically operates in the ISM bands (cell phones additionally use bands licensed by the operator), for example WiFi, Bluetooth and even microwave ovens, although this is not for communication. Typical devices are laptops, cell hpones, wireless routers and game consoles. More and more household appliances also use wireless connections to internet, going under the term “Internet Of things” (IOT).

Considering all the appliances in your house that uses wireless communication, and considering all your neighbor’s appliances that use wireless communication, the ISM band is starting to get crowded and communication is suffering due to “collisions”. And with the demand for faster communication/higher data rates some measures must be taken. Using additional frequencies is an obvious way to achieve this, only problem is most frequencies are already reserved for other uses.

Possible frequencies for wireless communications has a very wide span, but different frequencies/wavelengths also have different properties needing to be considered when selecting frequencies for specific tasks, and cost of necessary equipment for access to the selected frequencies may have

1.1 Cognitive Radio

Cognitive radio is based on the idea of monitoring the radio environment and utilizing the unused frequency resources for communication. Considering licensed bands, there is a primary user which is to be unaffected by opportunistic access schemes. The secondary user has to adapt to the use of the primary user and forfeit frequency resources immediately if any transmissions by the primary user is detected. Acting purely reactive is insufficient for proper utilization of the unused frequency resources, and a proactive approach creating/using a spectrum database[6] is necessary. Such a database could ideally be provided by the primary user, but a more real approach is to produce the maps based on on monitoring of the RF environment.

1.2 Radio Environment Maps

Spectrum cartography is the process of building spatial radio environment maps (REM) with regards to frequency and/or time.[1] REMs can be based on different parameters such as signal power, channel gains and interference, and used in several areas including network planning, frequency reuse, prediction of coverage, interference management, opportunistic spectrum access and cognitive radio.

Creating a spectrum map requires measurements done at known positions, and then filling in the space in-between and around these points using interpolation. For interpolation, a function with representative behavior as the original signal measured should be used, but seeing as these measured points tells nothing of the origin of the signal or environmental impacts on the signal, a standard off-the-shelf function is not applicable.

Best way to generate a representative radio environment map is to use function estimation for deciding on the function to use and necessary parameters to have it perform a suitable estimation.

2 Objective

The task at hand is to experimentally validate whether the algorithm presented in "Non-Parametric Spectrum Cartography using Adaptive Radial Basis Functions" produces functions that accurately estimates a spatial map of corresponding signal levels. And, attempt utilizing the produced function and it's properties for additional purposes.

Subsequently, the algorithm may be referred to as the "Radial Basis Function" or simply RBF

Different receiver configurations, different number of receivers, different number of transmitters and implementations in different development environments are used to discover possibilities and limitations of the algorithm. Along with a variety of custom developed functionality for visualizing measurements and results, processing and conditioning measurements and estimations, and adding extended functionality.

Radio frequency signal level information is gathered by sensors(RF receivers) along with the position of the sensors. Training of the function and validation of the results are done by randomly dividing RF measurements into two separate sets, the validation set and the training set. Number of measurements for each set should ideally be 80% for validation and 20% for training, but due to limited number of receivers a ratio of 50/50 have been used for most estimations.

Quality of the estimated function is mainly determined through Normalized Mean Square error, using the validation set and the estimated values at the position of the validation set sensors.

$$NMSE = E \left[\frac{\|h(x) - \hat{h}(x)\|^2}{\|h(x)\|^2} \right] \quad (1)$$

For improved readability the NMSE value is converted to decibel using $10 \cdot \log(NMSE)$

As this function is used to generate maps, a visual evaluation of resulting maps is also used to determine the validity.

3 Function estimation

Function estimation is the process of building a representative function for a limited known input/output data set.[5] Based solely on the known data, the created function should ideally be able to predict the correct output value for an unlimited number of input values.

3.1 One parameter

For the known scalar values: t and y

A possible function could be:

$$\hat{h}(x) = xa \tag{2}$$

Using the known dataset it can be found that:

$$a = \frac{y}{t} \tag{3}$$

Leaving the function:

$$\hat{h}(x) = x \cdot \frac{y}{t} \tag{4}$$

For any x .

3.2 Several parameters

Input for the function may also consist of several parameters, and one approach could be to supply a separate coefficient for each parameter.

Using vectors x and a the function could look like:

$$\hat{h}(x) = x^T \cdot a \tag{5}$$

$$\hat{h}(x) = [x_1 \quad x_2 \quad x_3] \cdot \begin{bmatrix} a_1 \\ a_2 \\ a_3 \end{bmatrix} \tag{6}$$

And considering four known sets (t, u, v, w) of multiple parameter input for four known output (y_1, y_2, y_3, y_4) values for function estimation, the function ideally is:

$$y = \Theta^T \cdot a \tag{7}$$

$$\begin{bmatrix} y_1 \\ y_2 \\ y_3 \\ y_4 \end{bmatrix} = \begin{bmatrix} t_1 & t_2 & t_3 \\ u_1 & u_2 & u_3 \\ v_1 & v_2 & v_3 \\ w_1 & w_2 & w_3 \end{bmatrix} \cdot \begin{bmatrix} a_1 \\ a_2 \\ a_3 \end{bmatrix} \tag{8}$$

But in real measurements, the corresponding a values may differ for the different input/output sets, and an approximation must be done to have the coefficients suit all the sets in a best possible way.

Acquiring the best values for the coefficients at this point is a bit more complex, but without going too much into details the estimated function can be written as a least squares estimation:

$$\hat{h}(x) = [x_1 \quad x_2 \quad x_3] \cdot \left(\begin{bmatrix} t_1 & u_1 & v_1 & w_1 \\ t_2 & u_2 & v_2 & w_2 \\ t_3 & u_3 & v_3 & w_3 \end{bmatrix} \cdot \begin{bmatrix} t_1 & t_2 & t_3 \\ u_1 & u_2 & u_3 \\ v_1 & v_2 & v_3 \\ w_1 & w_2 & w_3 \end{bmatrix} \right)^{-1} \cdot \begin{bmatrix} t_1 & u_1 & v_1 & w_1 \\ t_2 & u_2 & v_2 & w_2 \\ t_3 & u_3 & v_3 & w_3 \end{bmatrix} \cdot \begin{bmatrix} y_1 \\ y_2 \\ y_3 \\ y_4 \end{bmatrix} \quad (9)$$

Which basically corresponds to the previous formula rewritten as:

$$\hat{h}(x) = x^T \cdot (\Theta \cdot \Theta^T)^{-1} \cdot \Theta \cdot y \quad (10)$$

To smooth the estimated function, ridge regression can be applied by a regularization parameter lambda and an identity matrix

$$\hat{h}(x) = [x_1 \quad x_2 \quad x_3] \cdot \left(\begin{bmatrix} t_1 & u_1 & v_1 & w_1 \\ t_2 & u_2 & v_2 & w_2 \\ t_3 & u_3 & v_3 & w_3 \end{bmatrix} \cdot \begin{bmatrix} t_1 & t_2 & t_3 \\ u_1 & u_2 & u_3 \\ v_1 & v_2 & v_3 \\ w_1 & w_2 & w_3 \end{bmatrix} + \lambda \cdot \begin{bmatrix} 1 & 0 & 0 \\ 0 & 1 & 0 \\ 0 & 0 & 1 \end{bmatrix} \right)^{-1} \cdot \begin{bmatrix} t_1 & u_1 & v_1 & w_1 \\ t_2 & u_2 & v_2 & w_2 \\ t_3 & u_3 & v_3 & w_3 \end{bmatrix} \cdot \begin{bmatrix} y_1 \\ y_2 \\ y_3 \\ y_4 \end{bmatrix} \quad (11)$$

$$\hat{h}(x) = x^T \cdot (\Theta \cdot \Theta^T + \lambda \cdot I)^{-1} \cdot \Theta \cdot y \quad (12)$$

By applying identity: $(AB + \lambda I)^{-1}A = A(BA + \lambda I)^{-1}$ this can be rewritten as:

$$\hat{h}(x) = [x_1 \quad x_2 \quad x_3] \cdot \begin{bmatrix} t_1 & u_1 & v_1 & w_1 \\ t_2 & u_2 & v_2 & w_2 \\ t_3 & u_3 & v_3 & w_3 \end{bmatrix} \cdot \left(\begin{bmatrix} t_1 & t_2 & t_3 \\ u_1 & u_2 & u_3 \\ v_1 & v_2 & v_3 \\ w_1 & w_2 & w_3 \end{bmatrix} \cdot \begin{bmatrix} t_1 & u_1 & v_1 & w_1 \\ t_2 & u_2 & v_2 & w_2 \\ t_3 & u_3 & v_3 & w_3 \end{bmatrix} + \lambda \cdot \begin{bmatrix} 1 & 0 & 0 \\ 0 & 1 & 0 \\ 0 & 0 & 1 \end{bmatrix} \right)^{-1} \cdot \begin{bmatrix} y_1 \\ y_2 \\ y_3 \\ y_4 \end{bmatrix} \quad (13)$$

$$\hat{h}(x) = x^T \cdot \Theta \cdot (\Theta^T \cdot \Theta + \lambda \cdot I)^{-1} \cdot y \quad (14)$$

Rewriting the formula makes it depend on two inner products. The inner product of the estimation parameters and the known parameter set:

$$[x_1 \quad x_2 \quad x_3] \cdot \begin{bmatrix} t_1 & u_1 & v_1 & w_1 \\ t_2 & u_2 & v_2 & w_2 \\ t_3 & u_3 & v_3 & w_3 \end{bmatrix} \quad (15)$$

And the inner product of the known parameter set by itself:

$$\begin{bmatrix} t_1 & t_2 & t_3 \\ u_1 & u_2 & u_3 \\ v_1 & v_2 & v_3 \\ w_1 & w_2 & w_3 \end{bmatrix} \cdot \begin{bmatrix} t_1 & u_1 & v_1 & w_1 \\ t_2 & u_2 & v_2 & w_2 \\ t_3 & u_3 & v_3 & w_3 \end{bmatrix} \quad (16)$$

3.3 Kernel methods

Kernel methods depends on the known parameter set and the estimation parameters only through inner products.

$$k(x) = \begin{bmatrix} t_1 & t_2 & t_3 \\ u_1 & u_2 & u_3 \\ v_1 & v_2 & v_3 \\ w_1 & w_2 & w_3 \end{bmatrix} \cdot \begin{bmatrix} x_1 \\ x_2 \\ x_3 \end{bmatrix} \quad (17)$$

$$K = \begin{bmatrix} t_1 & t_2 & t_3 \\ u_1 & u_2 & u_3 \\ v_1 & v_2 & v_3 \\ w_1 & w_2 & w_3 \end{bmatrix} \cdot \begin{bmatrix} t_1 & u_1 & v_1 & w_1 \\ t_2 & u_2 & v_2 & w_2 \\ t_3 & u_3 & v_3 & w_3 \end{bmatrix} \quad (18)$$

Applying kernel methods to ridge regression leaves:

$$\hat{h}(x) = k(x)^T \cdot (K + \lambda I)^{-1} \cdot y \quad (19)$$

3.4 Gaussian Radial Basis functions

A radial basis function depends only on the distance from the origin. For a one-dimensional function $f(x)$ with origin at 0, the result would be the absolute value of x .

$$f(x) = \|x\| \quad (20)$$

For estimation, a radial basis function is typically extended with a weight value, a decay value and a position indicating the center of the RBF, and the sum of several radial basis functions provide the resulting estimation

$$f(x) = \sum_{k=0}^K \omega_k \cdot \|x - x_k\| \quad (21)$$

Extending this to a Gaussian Radial Basis Function, the result provides bell-shaped values depending on the distance from the origin and the decay parameter provided for the function.

$$f(x) = \sum_{k=0}^K \omega_k \cdot e^{-(\gamma_k \|x - x_k\|)^2} \quad (22)$$

3.5 Non-Parametric Spectrum Cartography using Adaptive Radial Basis Functions

The algorithm proposed by Mohamed Hamid[3] combines Kernel ridge regression with Gaussian radial Basis Functions as parameters for the estimation of radio environment maps.

The number of parameters for function estimation is a selected value representing number of centroids.

The estimatoin is based on a set of measured signals and the locations where they are acquired.

The radial basis function is adapted for use in spectrum cartography and to not to be too computationally expensive.

$$\hat{h}(x) = \omega_0 + \sum_{k=1}^K \omega_k \exp(-\gamma_k \|x - \mu_k\|^2) \quad (23)$$

Where:

\hat{h} is the estimated value at position x

ω_0 is a common weight for all centroids

K/k is total number of centroids/current centroid respectively

ω_k is the weight for the current centroid

γ_k is a decay parameter for the current centroid

μ_k is the position of the current centroid

In matrix form represented by:

$$\Theta \mathbf{w} = \mathbf{y} \quad (24)$$

$$\Theta = [\mathbf{1}_N | \theta], \theta \in R^{N \times K} \quad (25)$$

Θ is a $\mathbf{N} \times (\mathbf{K} + 1)$ matrix with the first column containing just ones, used both for estimation and training.

N is the number of estimations to perform, or the number of measurements used for training.

$$\theta_{nk} = \exp(-\gamma_k \|X_n - \mu_k\|^2), 1 \leq n \leq N, 1 \leq k \leq K \quad (26)$$

X_n is the position of estimated value number n , or the position of measurement number n for training.

For deciding the values of ω , γ and μ a test set is used.

To train \mathbf{w} ($\omega_0 + \omega_1 \dots \omega_k$) the following is formula is used:

$$\mathbf{w} = (\Theta^T \Theta + \lambda \mathbf{I}_K)^{-1} \Theta^T \mathbf{y} \quad (27)$$

I_K is a $K \times K$ identity matrix

$\Theta^T \Theta$ is the Gramian matrix of Θ

$\Theta^T \mathbf{y}$ is the moment matrix for a linear least squares approach to determine the values of \mathbf{w}

To train the γ parameter the following formula is used:

$$\gamma_k^i = \gamma_k^{i-1} - \alpha \sum_{n=1}^N \left((y_n - \hat{h}(x_n)) \cdot \|x_n - \mu_k\|^2 \cdot \omega_k \exp(-\gamma \|x_n - \mu_k\|^2) \right) \quad (28)$$

This adjusts the decay of the "signal" (positive or negative) which the centroid represents, fixing the steepness of the gaussian radial basis function. Illustrated in figure 2.

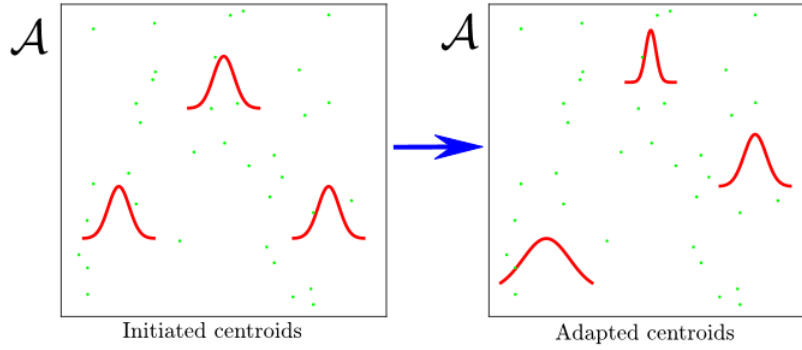


Figure 2: Adjusting steepness of bell curve for RBF

Represented in the map estimation as shown in figure 3:

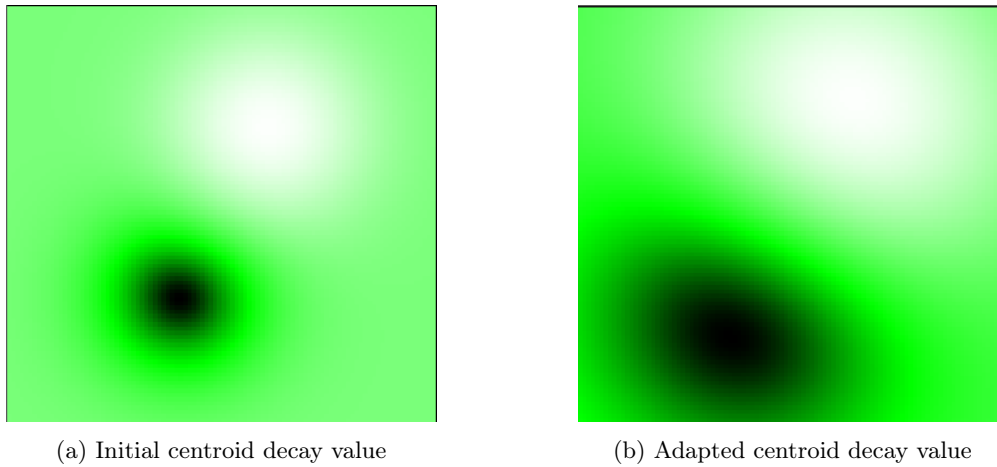


Figure 3: Adjustment of gamma values

Figure 3 shows an estimation for $K = 2$ centroids. ω_0 represents the green background, a negative and positive ω_k represents the black and the white area respectively.

To train the μ (centroid position) parameter the following equation is used:

$$\mu_k^i = \mu_k^{i-1} + 2\alpha\gamma_k \sum_{n=1}^N \left((y_n - \hat{h}(x_n)) \cdot (x_n - \mu_k) \cdot \omega_k \exp(-\gamma_k \|x_n - \mu_k\|^2) \right) \quad (29)$$

The value for α is initially chosen, and must be adjusted depending on the initial parameters and the received signal strength. Using too high a value causes γ_k to get negative values, causing the estimation to stop or producing anomalous artifacts on the spectrum map. With too small α the changes produced for the map are so small that it is not observable that there are any changes during the iterations. The initial value for γ is also selected and experimentally it works best at between 0.1 and 0.3.

Training the parameters requires a set of measurements. The measurements are arranged in clusters consisting of several measurements each. The initial selection for the clusters is performed in a counter-clockwise quadrant based order. First cluster consists of measurements closest to the coordinate (0,0), the second cluster consists of measurements closest to the coordinate (max-x, 0) and so on until all measurements are assigned to a cluster.

The initial positions for the centroids (μ) representing the clusters are based on the average of the positions for the measurements in the cluster.

With the centroids initialized, a finite set of iterations for \mathbf{w} , γ and μ is performed in this order.

4 Detection of signal presence

For real life applications, in order to create representational spectrum maps, it is essential to know whether there is a signal present in the measurements used for estimation. This can be achieved using energy detection (ED)[7][4].

For a N sized vector of measurements X

$$\sum_{j=1}^N |x_j|^2 < \rho \quad (30)$$

Where ρ is the detection threshold value. Decision for this value can be based on a function for the probability of false alarm (Pf).

$$P_f = Q\left(\frac{\rho - N\sigma_z^2}{2\sqrt{2N}\sigma_z^2}\right) \quad (31)$$

With σ_z^2 being the noise variance and Q complementary cumulative distribution function of a Gaussian random process.

Solving for ρ gives the threshold for a specified value for Probability of false:

$$\rho = \sqrt{2N}\sigma_z^2 Q^{-1} P_f + N\sigma_z^2 \quad (32)$$

Where Q^{-1} is the inverse Q function.

Base on this the probability of detection for the energy detector is given by:

$$P_d = Q\left(\frac{\rho - N(\gamma_0 + 1)\sigma_z^2}{2\sqrt{2N}(\gamma_0 + 1)\sigma_z^2}\right) \quad (33)$$

Where γ_0 is the received Signal to noise ratio

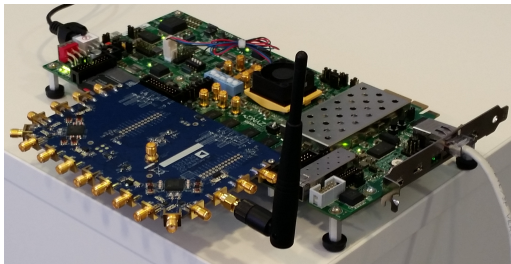
For the measurements done in this project, signal presence is assumed to be constant as the transmitting source is controlled manually. Thus ED has not been implemented as part of the estimation functionality.

5 Sequential measurements using 1 transmitter and 1 receiver

Initial testing has been performed with the Radial Basis function[2] using only one receiver and registering measurements sequentially on an evenly spaced grid layout. The transmitter is placed within the boundaries of the receiver grid.

5.1 Equipment and setup

The setup consists of a USRP-2953R for transmitting a RF signal, a custom software defined radio (SDR) using Xilinx ZC706 with a FMCOMMS5 transceiver for receiving the signal, and a laptop for registering the signal from the receiver. The laptop also generates the signal to be sent from the transmitter. All devices are connected via a 100Mb/s switch using wired Ethernet.



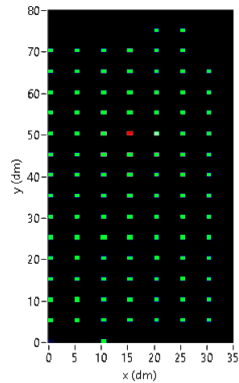
(a) Xilinx ZC706 with FMCOMMS5



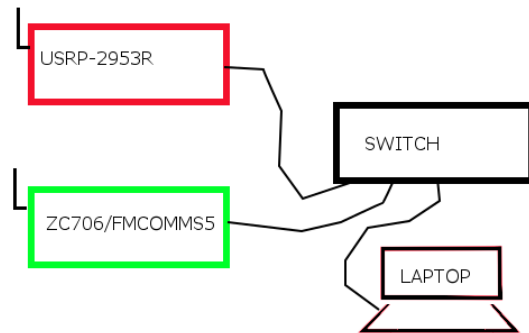
(b) NI USRP 2953R

Figure 4: Equipment

The transmitter, represented by red color in figure 5, is placed at a fixed position while the receiver, green color, is moved to each green location for measurements to be registered.



(a) Transmitter and receiver locations



(b) Transmitter, receiver and laptop connectivity

Figure 5: Setup of test system

5.2 Implementation in NI LabView

Due to the measurements being performed sequentially, a virtual instrument (VI) has been created that calculates the mean variance over some time. 10.000 samples are retrieved from the receiver and the variance is calculated and plotted in a graph. The next iteration calculates the variance again, and the mean value of the collected variances is plotted. This calculation and plotting runs continuously until the 100 last plotted mean variances does not differ by more than a threshold value of 0.01 dB. Whereas the measurements result is stored in an array along with the position of the receiver, and the array is written to a file. Figure 6 shows the main loop of the signal registration process.

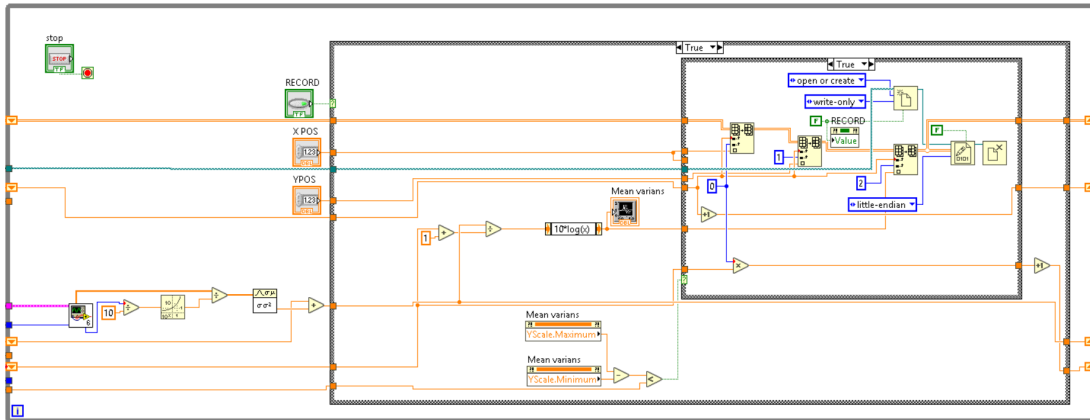


Figure 6: Signal registration - Main loop

To generate the values for the weight \mathbf{W} , the following is implemented:

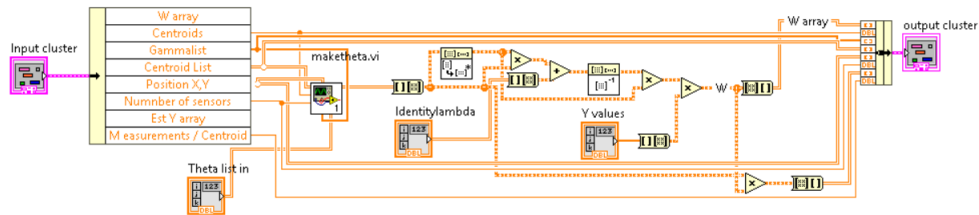


Figure 7: LabView Implementation of formula for generating \mathbf{W}

For training the γ parameter the above mentioned formula is implemented as:

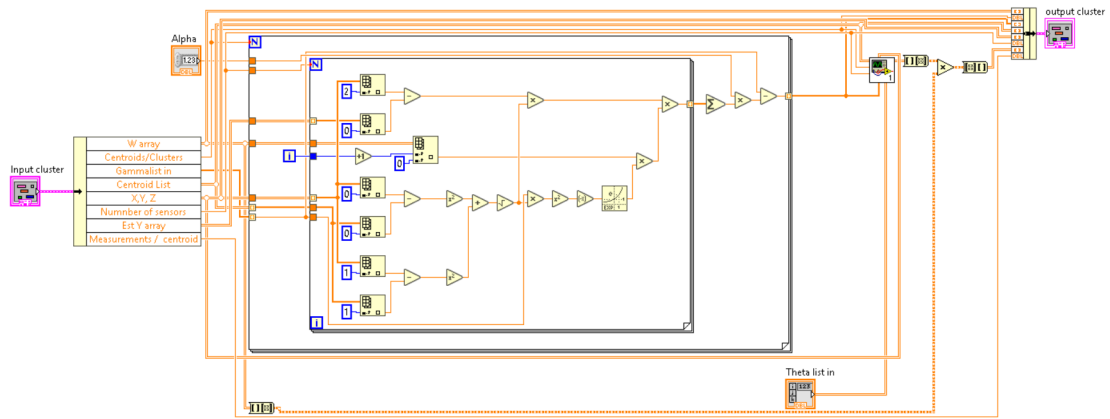


Figure 8: LabView implementation of formula for adjusting γ

To optimize the centroid positions μ , the implementation is:

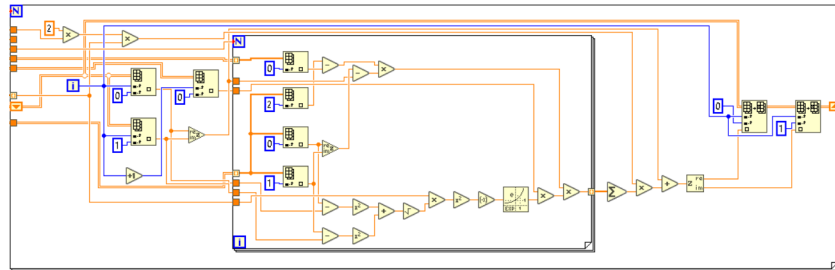
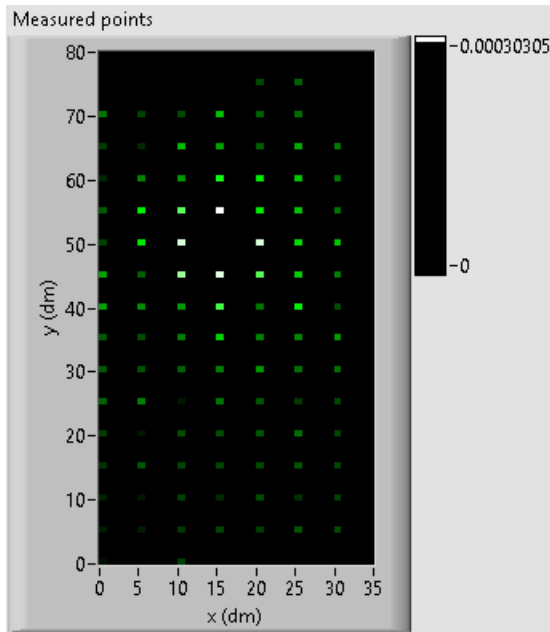


Figure 9: LabView implementation of formula for adjusting centroid positions μ

5.3 Measurements and estimation

Measurements are performed in an unshielded office environment. Tiles on the floor (0.5m x 0.5m) is used for spatial reference. The signal is transmitted on 5,41 GHz with at a sample rate of 1 MSPS using binary phase shift keying. Receiving node uses a sample rate of 3 MSPS and 3 MHz bandwidth. Measurements are performed sequentially, due to limited resources. To account for the measurements not being simultaneous, the mean variance over a short time span has been used. During the time period of which the measurements was taken, the environment was kept as uniform as possible. But some anomalies was observed, probably due to the presence of the operator and reflections caused by the metal in a chair used by the operator.



(a) Mapped measurements



(b) Measuring

Figure 10: Registering measurements

For a proper test of the algorithm, a random selection of twenty measurements is reserved for the training part, while the remaining 80 measurements are used for verification and comparison to the estimated map.

Using ten centroids and only the average position of two measurements to initially define the centroid positions.

The estimation is performed for a 35x80 (dm) map area, representing the area in which the measurements were taken.

Comparing the estimated values to the measured values a normalized mean square error (NMSE) of -7.67 dB is attained.

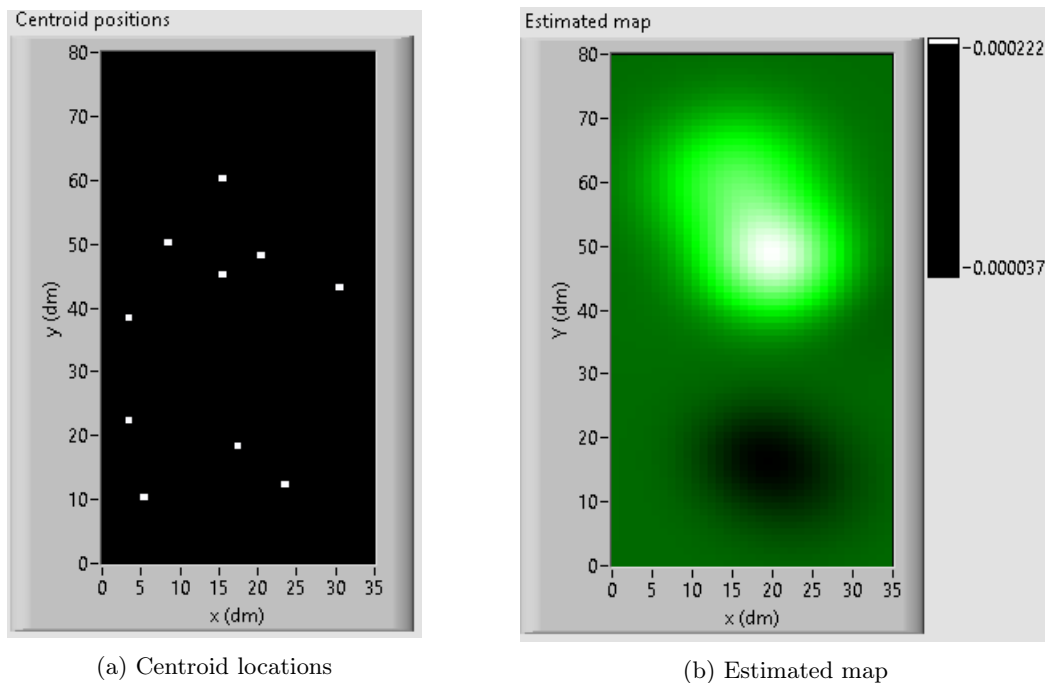


Figure 11: Estimation based on sequential measurements

6 Parallell measurements using 14 receivers and 1 transmitter

6.1 Equipment

6.1.1 NI USRP-2953R & NI USRP-2952R

Both contains 2 transceivers, has 40 MHz bandwidth and supports GPS disciplined clock, but differs in frequency range.



Figure 12: NI USRP 2953R 1.2 GHz-6GHz



Figure 13: NI USRP 2952R 400MHz-4.4GHz

6.1.2 NI PXIe-1082 & NI PXIe-1071

PXI chassis having extended operating temperature, speeds up to 8GB/s.



Figure 14: NI PXIe 1082 - 8 slots

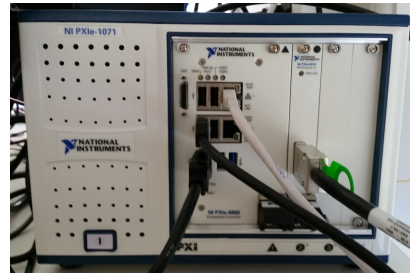


Figure 15: NI UPXIe 1071 - 4 slots

6.1.3 NI PXIe-8880



- PXI controller
- Intel Xeon 8-core processor
- 2.3GHz
- 24 GB RAM
- 2 x 10/100/1000 BASE-TX(Gigabit) Ethernet ports
- 2 x USB 3.0 ports
- 4 x USB 2.0 ports
- Integrated harddrive
- Serial port
- Other peripheral I/O

Figure 16: NI PXIe8880

6.1.4 NI PXIe-8374 extension card

Provides PCI Express X4 interface for USRPs.



Figure 17: NI PXIe 8374

6.1.5 NI Linux Real-Time OS

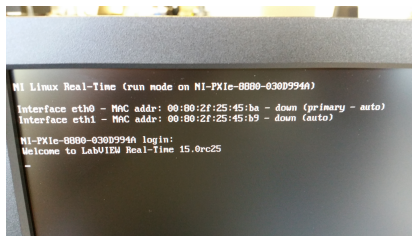


Figure 18: NI Linux Real-Time OS

- Runs on the PXIe-8880 controller
- Provides remote access for Communications Suite 2.0
- Improvement for time critical operations

6.1.6 Ni LabVIEW Communications System Design Suite 2.0

Visual design environment for doing digital signal processing, creating software for FPGA or real-time targets and/or prototyping communication systems. Has built-in support for NI devices. Frameworks, reference-designs and tutorials are available in software and online to quickly get started creating state-of-the-art communication designs.

6.2 Implementation in Communications Suite 2.0

Implementation is done in Communications suite 2.0. Several modules are created to retrieve, process and present the results. Queuing is used to have the different processes independent of each other, and all processes are configured to run simultaneous.

6.2.1 Signal registration

Registers the received signal within specified bandwidth on 14 RF receivers. Calculates the standard deviation of the received signals and queues this value along with the position of the receivers for further.

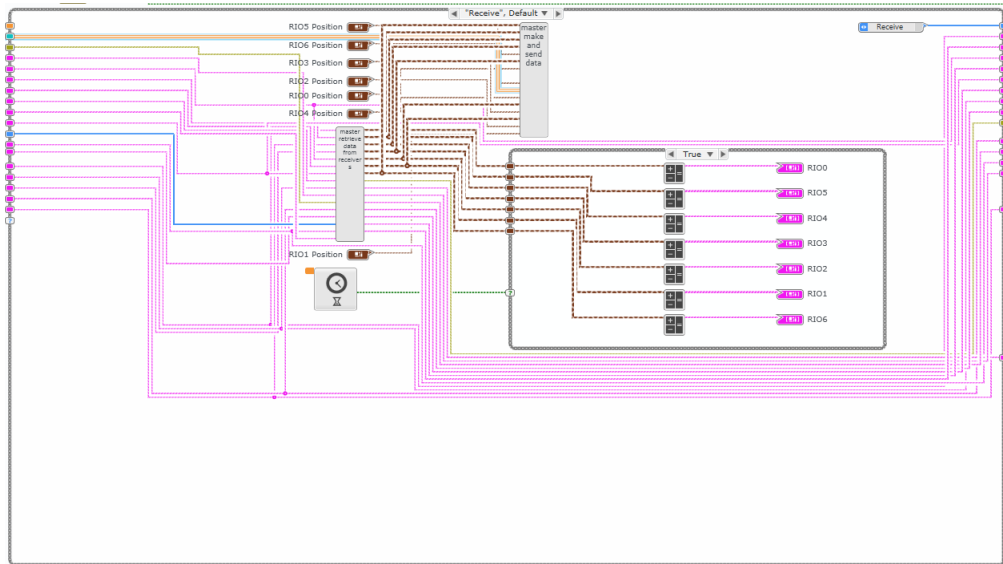


Figure 19: Implementation of receiving and conditioning of received signal

The main loop implementation for Communications Suite 2.0 is shown in figure 19, while figure 20 show a power density spectrum example for both channels (blue/red) on each USRP.

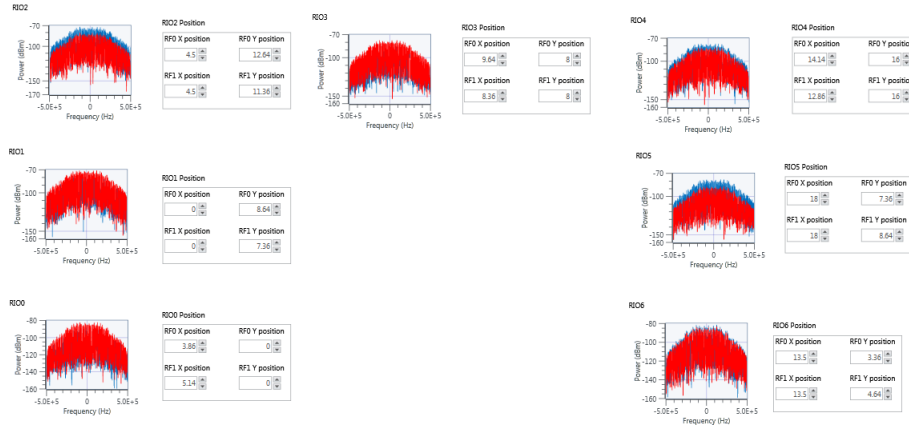


Figure 20: Panel visualization of received signal for all receivers

6.2.2 Adaptive Radial Basis Function

Recreates the spectrum map based on measurements using RBF algorithm. Figure 21 shows the main loop for the training part of the algorithm. First the weights (W) are generated, then the gamma values are processed and lastly the positions are modified.



Figure 21: Main loop of RBF estimation

Figure 22 is a top level illustration of how the training part for W (ω) is implemented.

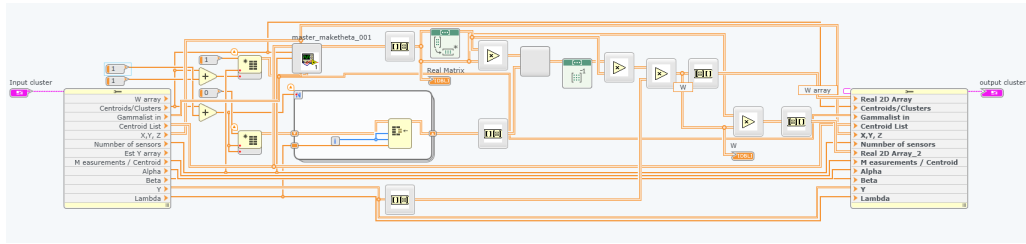


Figure 22: Conditioning the weight parameters

Implementation of conditioning of the gamma (γ) parameters is shown in figure 23.

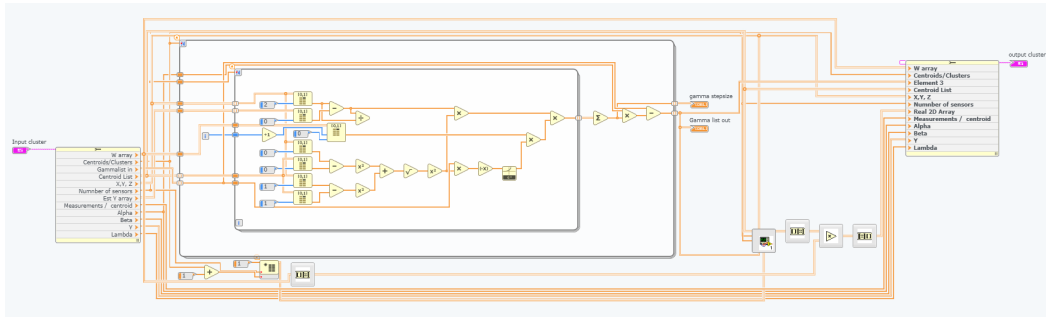


Figure 23: Conditioning the γ parameters

And implementation for modifying the centroid positions (μ) is shown in figure 24.

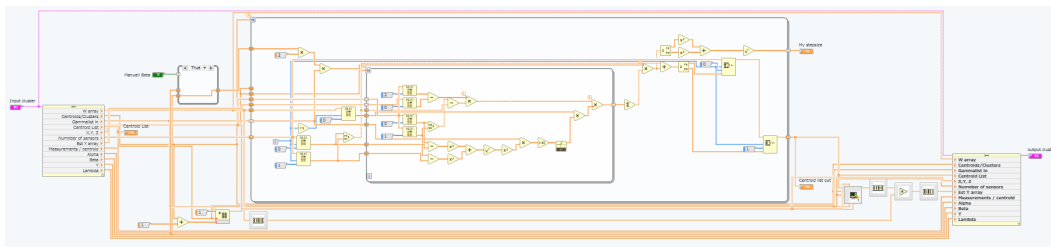


Figure 24: Conditioning of the μ parameter

6.3 Setup of measurement array

An array consisting of seven NI USRP 2953R is placed in specific locations and connected to NI PXIe-8374 extension cards in the PXIe-1082 using PCI Express X4 interface. Figure 25 shows an example of the placement of all the USRPs used for receiving. This setup is currently only used for trying to locate a transmitter outside of the receiver array.

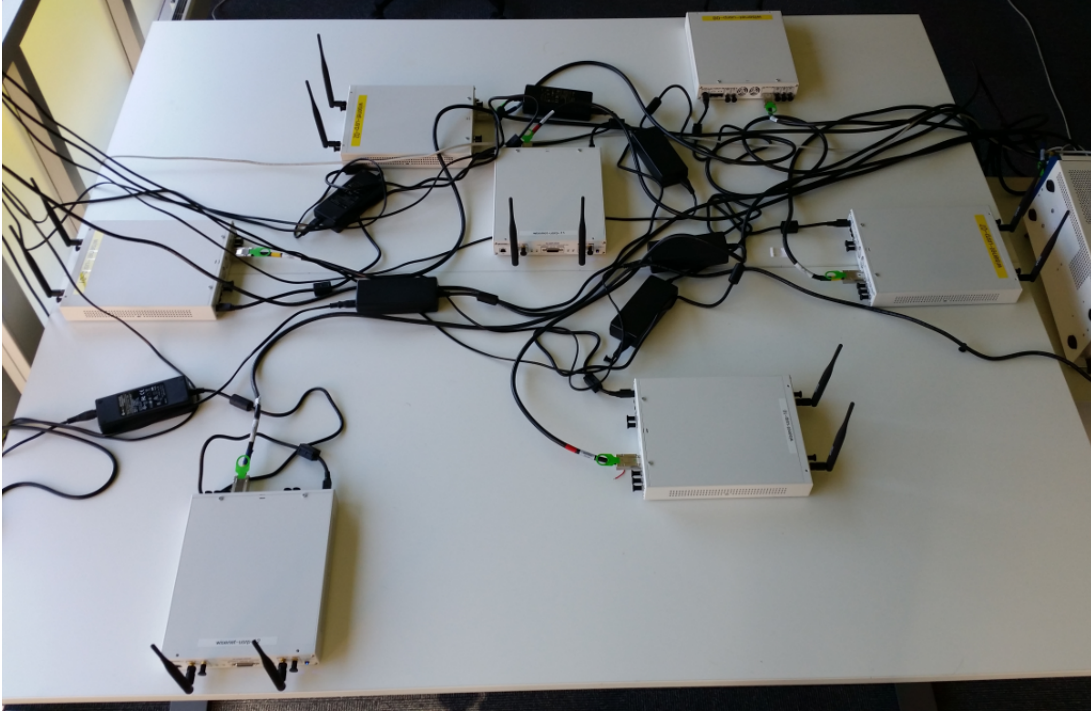


Figure 25: Placement of receivers

NI USRP 2952R is used as transmitter. This is connected to the NI PXIe-1071 using wired ethernet. The transmitter is shown in the upper leftmost corner of figure 26, along with the receiver array placed on the table. The chassis next to the table is the PXIe-1082 to which all the receiving USRPs are connected.



Figure 26: Test setup

Measurements are normally performed using all 14 receivers, which are divided into 2 sets of 7 receivers each, one set for training the function and one separate set for validating the resulting function. Sensors for the sets are selected randomly.

6.4 Estimation with one transmitter inside receiver array

A visualized example of measurements with one transmitter present is shown in figure 27. The transmitter is not marked in the figure but is positioned at coordinate (33.36,41).

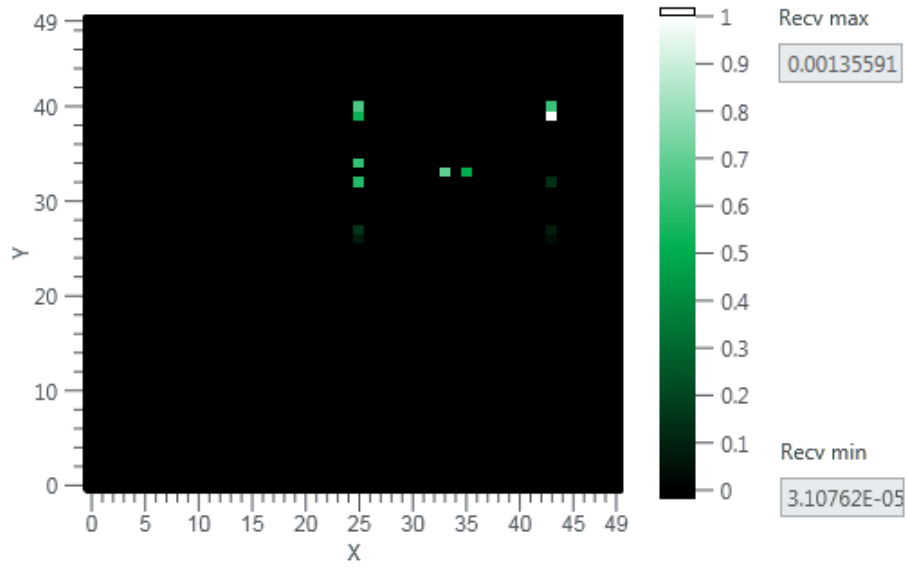


Figure 27: Estimation with transmitter inside array

Doing 1000 measurements with all receivers, randomly selecting 7 of the receivers for training and 7 for verification each time measuring is performed, the following results are produced. Estimated map in figure 28 represents the map with best NMSE of the 1000 maps generated from the measurements.

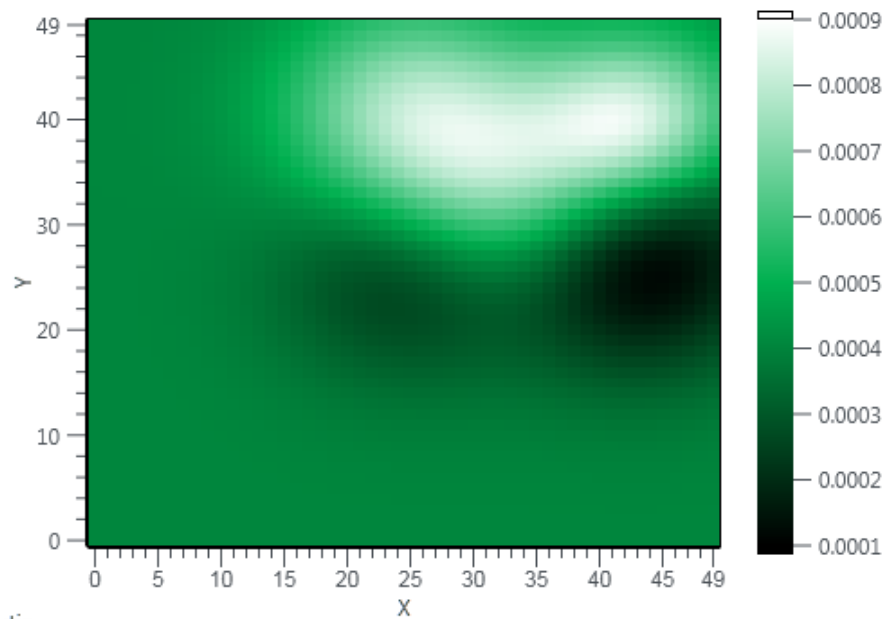


Figure 28: Estimation with transmitter inside array

| Centroid | W | Gamma | X pos | Y pos |
|----------|-----------|-----------|----------------|-------|
| (0) | 4.07E-04 | - | - | - |
| 1 | -2.76E-04 | 0.0984846 | 43 | 25.5 |
| 2 | -9.66E-05 | 0.949093 | 43 | 32.36 |
| 3 | 5.03E-04 | 0.122954 | 43 | 29.22 |
| 4 | 3.54E-04 | 0.0999965 | 25 | 40.5 |
| 5 | 3.44E-04 | 0.100133 | 33.36 | 33 |
| 6 | -7.04E-05 | 0.103781 | 43 | 33.64 |
| 7 | -2.09E-04 | 0.100002 | 25 | 25.5 |
| Max NMSE | Min NMSE | Mean NMSE | NMSE Std. Dev. | |
| 5.09259 | -16.1611 | -6.01446 | 2.3268 | |

Table 1: Results of estimation with transmitter inside array

6.5 Estimation with one transmitter outside of receiver array

To assess the possibilities of the estimation algorithm, a transmitter is placed at position (25 , 51). Slightly above the center of the mapped area, and outside of the receiver array. In figure 29 the green squares represents receivers while the red square is the transmitter.

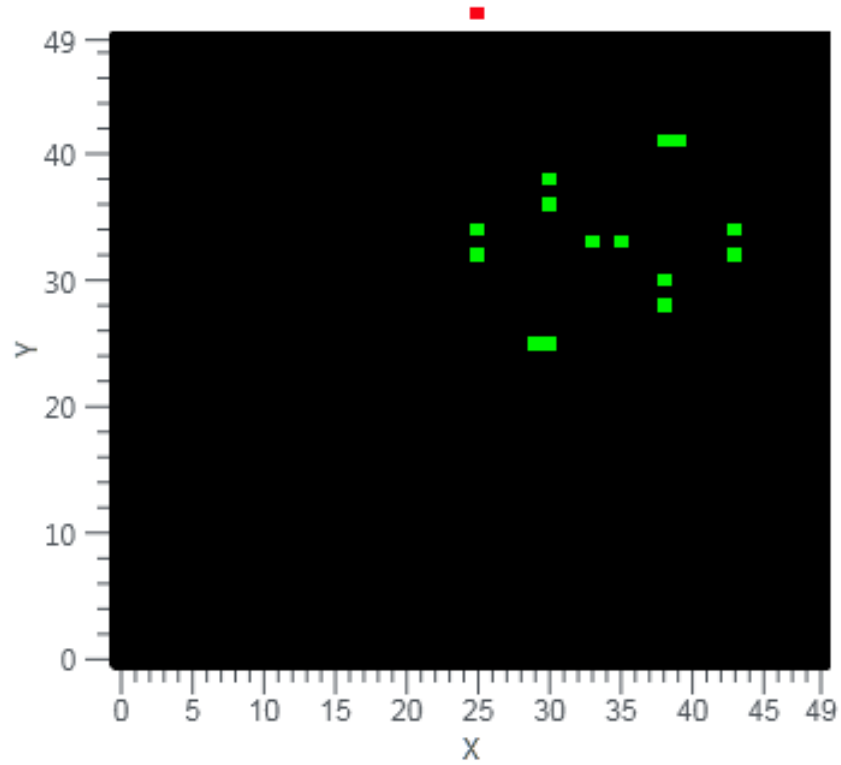


Figure 29: Placement of transmitter and receivers

This measurement is performed 1000 times, each time producing a map based on 1000 iterations of the RBF algorithm. Below in figure 30 the map which represents the best NMSE value achieved during testing is shown. As NMSE is presented in decibel, and NMSE represents the difference between the measured values and estimated values, a higher negative value is favorable.

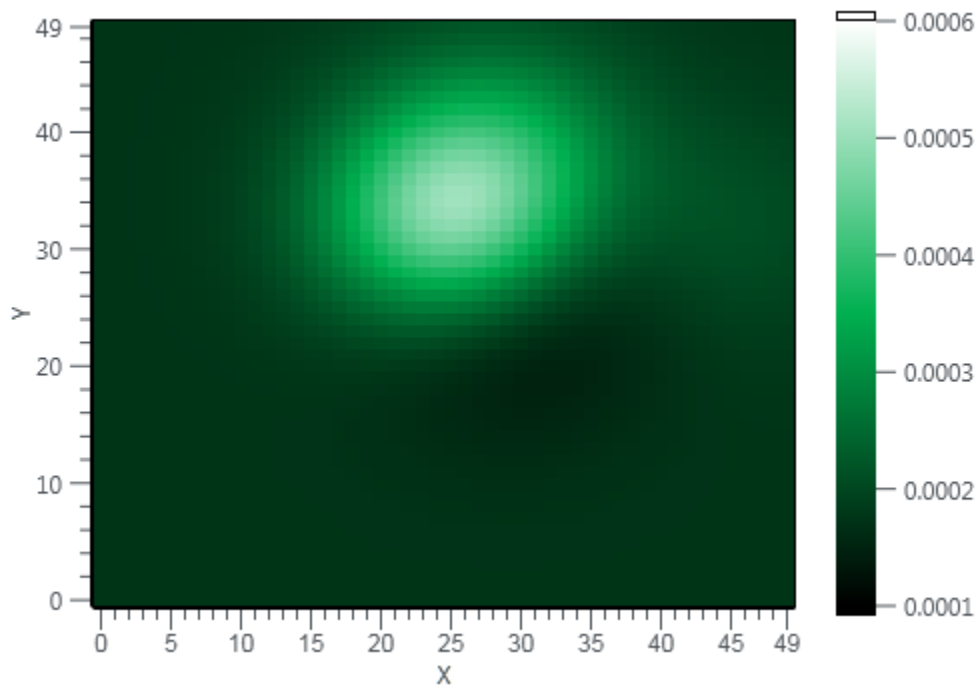


Figure 30: Estimation with transmitter outside receiver array

| Centroid | W | Gamma | X pos | Y pos |
|----------|--------------|-----------|----------------|---------------|
| (0) | 0.000174313 | - | - | - |
| 1 | -1.0098E-05 | 0.999897 | 37.86 | 41 |
| 2 | 5.31777E-05 | 0.100145 | 43 | 32.36 |
| 3 | -7.39022E-05 | 0.0962679 | 34.63988 | 33.00007 |
| 4 | 7.67054E-05 | 0.108119 | 29.49992 | 37.6415 |
| 5 | 0.000101205 | 0.0833626 | 29.4996 | 36.3611 |
| 6 | 0.000262915 | 0.112226 | 24.99653016 | 32.35974 |
| 7 | -7.16308E-05 | 0.100468 | 28.86001 | 24.9999899128 |
| Max NMSE | Min NMSE | Mean NMSE | NMSE Std. Dev. | |
| 1.93174 | -13.2852 | -6.21195 | 2.06794 | |

Table 2: Results for estimation with transmitter outside receiver array

Observation:

As the transmitter is placed apart from the receiver array, and centroids barely move beyond boundaries set by receiver positions, the transmitter is not clearly located and the map merely indicates the direction of the transmitter.

The results presented is automatically evaluated based on NMSE, but this does not necessarily mean that the estimation is a representational map for the signal levels in the estimated area. The algorithm does its best to fit the function to the measurements and sometimes produces "inversed" maps, meaning signal is considered to be omni-present and the fitting simply creates "holes" accommodating the levels of the sensors, illustrated in figure 31.

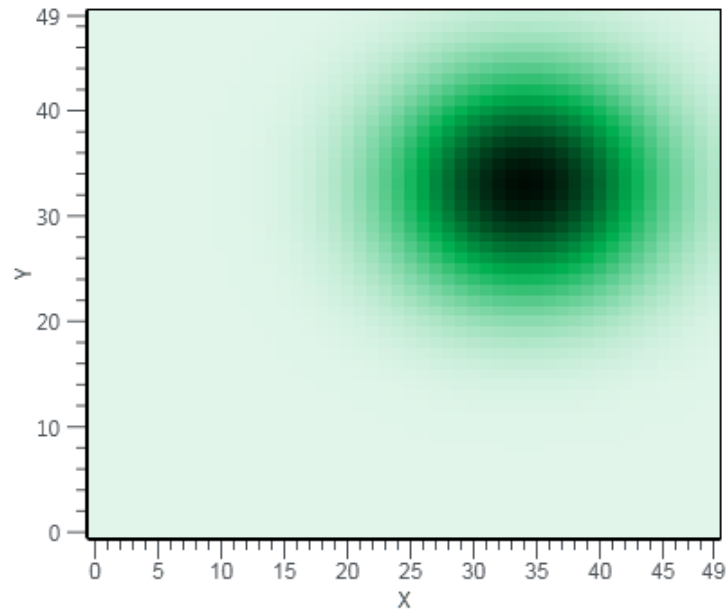


Figure 31: Example of inversed map

6.6 Estimation based tracking of one transmitter

As an attempt to utilize the properties of the estimated RBF, functionality is implemented in order to track the position of a transmitter based on the RBF centroids positions.

Using the position of the centroid with the highest weight value, new centroid positions are "weighed", adding only 0.1 of the distance from the current suggested transmitter location position to the new position of the centroid in order to provide a more stable location. In Figure 32 the transmitter is mapped as it is moved alongside the array of receivers. The amplitude represents number of positions that has been acquired, effectively displaying the movement of the transmitter over time.

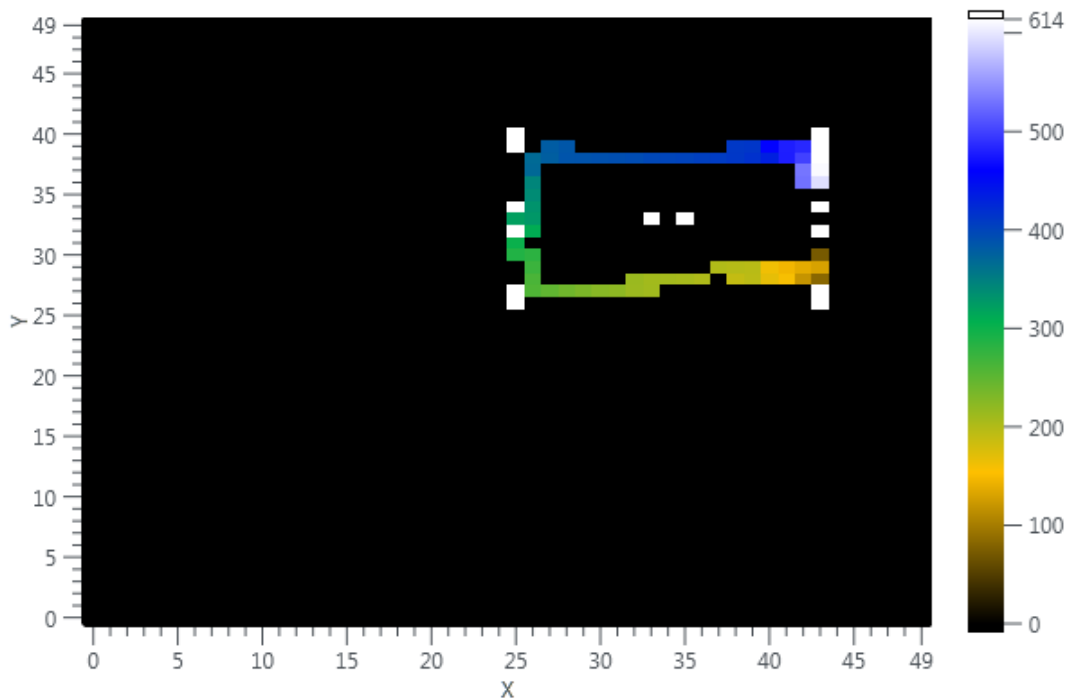


Figure 32: Tracking transmitter

7 Parallell measurements with an added transmitter

Equipment is the same as for the previous measurements with the addition of 1 USRP 2952R used as an additional transmitter

7.1 Estimation for multiple transmitter setup

Figure 33 shows an example of measurements of two transmitters. Transmitters are not marked in the figure but are located at $(33.36, 41)$ and $(33.36, 25)$.

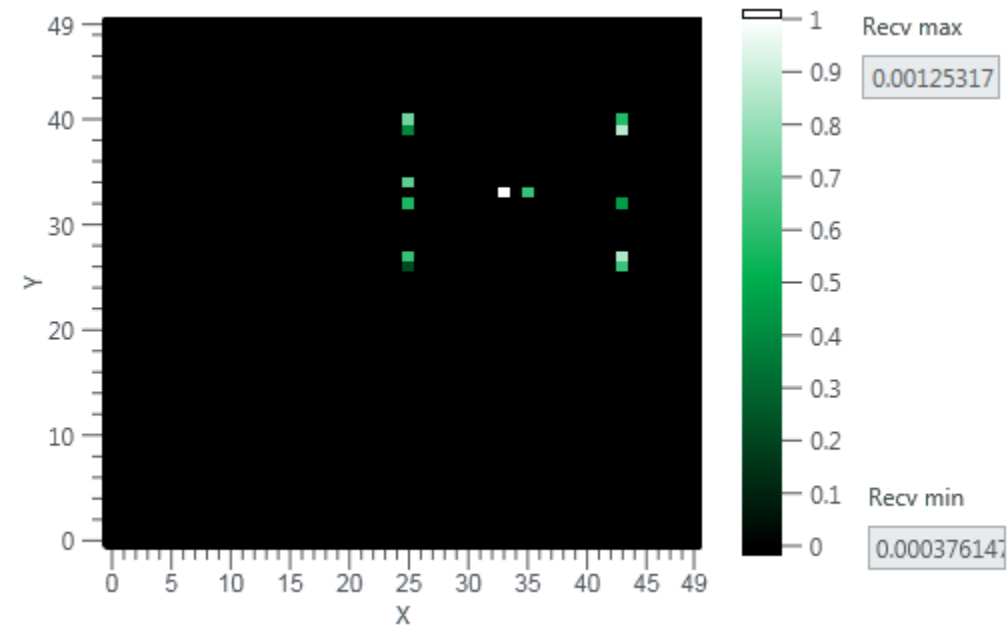


Figure 33: Received signal for 2 transmitters

To get some sense of how well the RBF algorithm performs with 2 transmitters present, 1000 maps are created. Each map done by 1000 iterations.

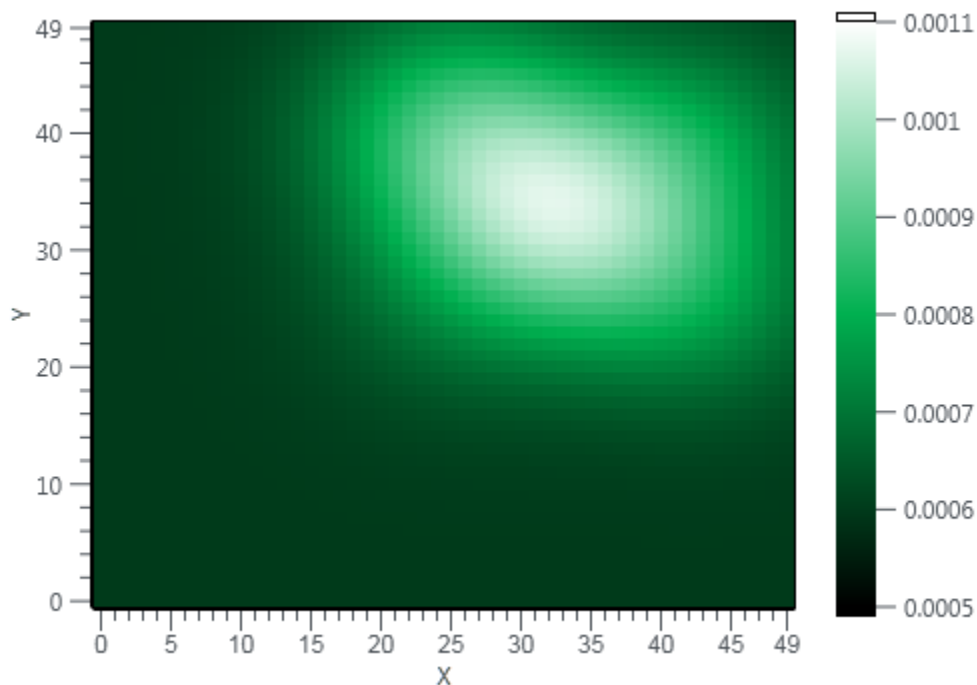


Figure 34: 1000 maps for 2 transmitters - Best NMSE

| Centroid | W | Gamma | X pos | Y pos |
|----------|--------------|-----------|-------------------|-----------|
| (0) | 0.000599534 | - | - | - |
| 1 | 2.17366E-05 | 0.0995546 | 25.00000000234274 | 25.500069 |
| 2 | 0.000328026 | 0.100121 | 33.36 | 33 |
| 3 | 0.000139672 | 0.108512 | 43 | 39.2203 |
| 4 | 0.000230713 | 0.099982 | 25.0000000242768 | 40.5 |
| 5 | 5.00602E-05 | 0.101444 | 25.0000000300467 | 26.78023 |
| 6 | -4.81757E-05 | 0.102391 | 43 | 33.63994 |
| 7 | 0.000154256 | 0.103034 | 43 | 26.77991 |
| Max NMSE | Min NMSE | Mean NMSE | NMSE Std. Dev. | |
| -4.87264 | -16.842 | -9.05326 | 1.70194 | |

Table 3: Best results for 1000 maps with 2 transmitters

7.2 Estimation based tracking of multiple transmitters

Functionality for tracking transmitters is extended to identify and track different transmitters based on centroid locations. The position of centroids with weight above a selected threshold value is compared to a table containing possible transmitter locations. If the centroid is within a certain range of one of the entries, it is considered to be the same transmitter and the stored position is updated using 0.1 of the distance between the centroid position and the current transmitter location. For each possible transmitter location there is a "timeout" value which is continuously decreased, but reset to a specified value each time the position is updated. As long as the possible transmitter location does not time out, a "life" value is continuously increased. The stored data for 2 located transmitters is shown in figure 34.

| Transmitter | X | Y | Timeout | Life |
|-------------|----|---------|---------|------|
| 1 | 25 | 38.4165 | 20 | 1912 |
| 2 | 43 | 28.5947 | 19 | 1912 |

Table 4: Stored tracking data for multiple transmitters

Due to the current setup with a limited number of receivers, tracking is currently limited to movement along the Y axis on either side of the receiver array. Movement along the X axis is not possible as there is only one receiver in the middle, and the functionality is unable to decide which transmitter is moving. Figure 35 shows the movement of both transmitters along the Y axis.

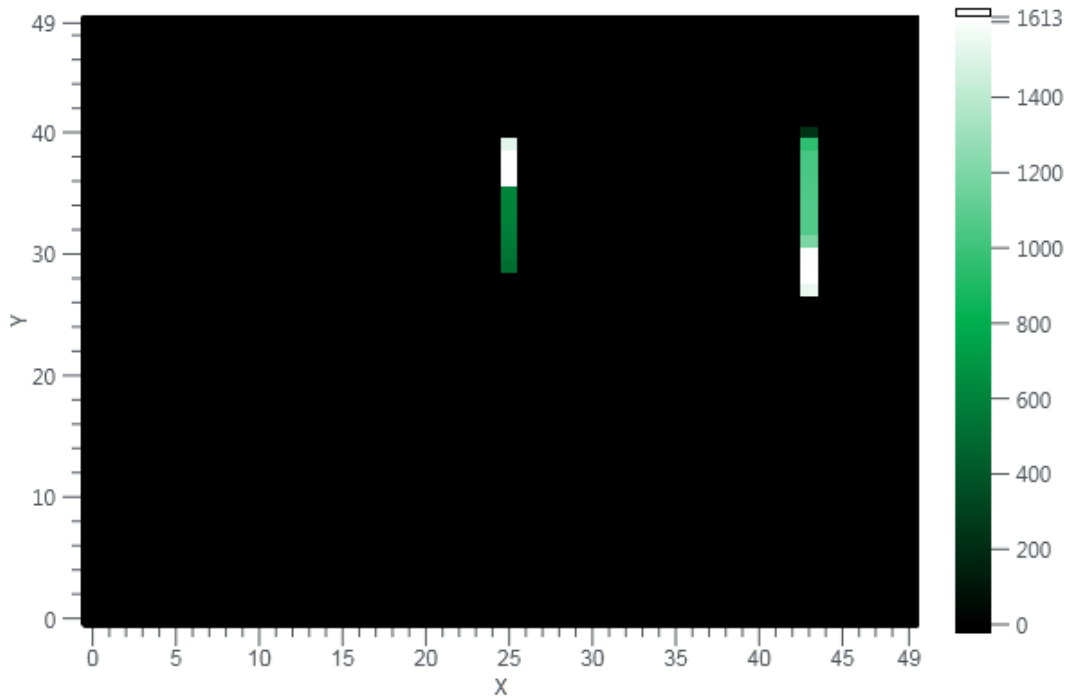


Figure 35: Tracking multiple transmitters

8 Conclusion

Experimenting with the RBF algorithm is interesting as it does produce maps based on the measured signal levels. The weight values and the decay values adapts to the received signal and the position of the belonging centroid, but the position adaption for the centroids is not optimal. Representative maps are created if the transmitter is close to one of the measurement points and inside of the receiver array, but if the transmitter is beyond the "boundaries" shaped by the receivers, or the receivers are spaced too far apart the results tends to be very inaccurate.

The *alpha* value has to be adjusted to "fit" the received signal levels, too low value gives very little change for each iteration, and too high value causes the decay value λ to go negative. With negative λ , the exponential function in the gaussian radial basis function suddenly has a positive parameter, and frequently produces infinite values causing the algorithm to break. Although the α value is fitted for adapting the decay value, this value is too small to have much effect on adapting the centroid positions.

Regardless, the ridge regression used for finding \mathbf{W} , makes it possible to use the centroids and their weights to locate and track at least one transmitter inside of the receiver array, possibly multiple transmitters if used with a larger array of receivers and/or a more optimized tracking function.

9 References

- [1] W.R Wu D. H. Huang, S. H. Wu and P. H. Wang. Cooperative radio source positioning and power map reconstruction: A sparse bayesian learning approach. *IEEE Trans. Veh. Technol.*, vol 64, issue 6, pp. 2318 - 2332, 2015.
- [2] T. Jordbru L. R. Cenkeramaddi-B. Beferull-Lozano H. Idsøe, M. Hamid. Spectrum cartography using adaptive radial basis functions: Experimental validation. *Accepted for IEEE SPAWC 2017*, 2017.
- [3] B. Hamid, M.; Beferull-Lozano. Non-parametric spectrumcartography using adaptive radial basis functions. *Accepted for ICASSP 2017*, 2016.
- [4] M. Hamid. *On Spectrum Sensing for Secondary Operation in Licensed Spectrum*. KTH Royal Institute of Technology, 2015.
- [5] D. Romero. Lecture notes in function estimation, 2017.
- [6] S. Bhattacharjee S. Debroy and M. Chatterjee. Spectrum map and its application in resource management in cognitive radio networks. *IEEE Trans. Cognitive Commun. and Networking*, vol 1, no 4, pp 406-419, December 2015.
- [7] L. R. Cenkeramaddi B. Beferull-Lozano H. Hamid T. Jordbru, H. Idsøe. Radios measurements on a customized software defined radio module: A case study of energy detection spectrum sensing. *Accepted for I2MTC 2017*, 2017.

List of Figures

| | | |
|----|--|----|
| 1 | Spectrum Allocation for norway (Source:NKOM) | 4 |
| 2 | Adujusting steepnes of bell curve for RBF | 11 |
| 3 | Adjustment of gamma values | 11 |
| 4 | Equipment | 14 |
| 5 | Setup of test system | 14 |
| 6 | Signal registration - Main loop | 15 |
| 7 | LabView Implementation of formula for generating \mathbf{W} | 15 |
| 8 | LabView implementation of formula for adjusting γ | 16 |
| 9 | LabView implementation of formula for adjusting centroid positions μ | 16 |
| 10 | Registering measurements | 17 |
| 11 | Estimation based on sequential measurements | 18 |
| 12 | NI USRP 2953R 1.2 GHz-6GHz | 19 |
| 13 | NI USRP 2952R 400MHz-4.4GHz | 19 |
| 14 | NI PXIe 1082 - 8 slots | 19 |
| 15 | NI UPXIe 1071 - 4 slots | 19 |
| 16 | NI PXIe8880 | 20 |
| 17 | NI PXIe 8374 | 20 |
| 18 | NI Linux Real-Time OS | 20 |
| 19 | Implementation of receiving and conditioning of received signal | 21 |
| 20 | Panel visualization of received signal for all receivers | 22 |
| 21 | Main loop of RBF estimation | 22 |
| 22 | Conditioning the weight parameters | 23 |
| 23 | Conditioning the γ parameters | 23 |
| 24 | Conditioning of the μ parameter | 23 |
| 25 | Placement of receivers | 24 |
| 26 | Test setup | 25 |
| 27 | Estimation with transmitter inside array | 26 |
| 28 | Estimation with transmitter inside array | 27 |
| 29 | Placement of transmitter and receivers | 28 |
| 30 | Estimation with transmitter outside receiver array | 29 |
| 31 | Example of inversed map | 30 |
| 32 | Tracking transmitter | 31 |
| 33 | Received signal for 2 transmitters | 32 |
| 34 | 1000 maps for 2 transmitters - Best NMSE | 33 |
| 35 | Tracking multiple transmitters | 34 |

List of Tables

1 Results of estimation with transmitter inside array 27
2 Results for estimation with transmitter outside receiver array 29
3 Best results for 1000 maps with 2 transmitters 33
4 Stored tracking data for multiple transmitters 34